Analysis and Prediction of Coastal Erosion Status Based on Multisource Remote Sensing Data —A Case Study of Fangchenggang

Runjie Wang,[1,2]* Junyv Kang,[1] Liyuan Hou,[3] and Xiao Zhang[1]

[1]School of Geomatics and Urban Spatial Informatics, Beijing University of Civil Engineering and Architecture,
No. 1, Zhanlanguan Road, Beijing 100048, PR China
[2]Beijing Key Laboratory of Urban Spatial Information Engineering,
No. 15, Yangfangdian Road, Beijing 100038, PR China
[3]Land Surveying and Mapping Institute of Shandong Province, Shandong Jinan 250013, PR China

The analysis and prediction of the coastal erosion status are of great significance for maintaining the marine ecological environment, planning urban construction, and coping with climate change. Fangchenggang is located in the southwesternmost part of mainland China. It has the largest harbor in the western region, which provides access to the most convenient channel between southwest China and the Association of Southeast Asian Nations. With the rapid development of China's economy, coastal erosion has occurred in Fangchenggang, and ecological and environmental problems have become increasingly prominent. In this study, we mainly focus on the status analysis and prediction of Fangchenggang coastal erosion based on multisource remote sensing data. A systematic analysis and prediction methods for the coastal erosion state are studied. First, shoreline type changes are analyzed. The index of coastline type diversity is used instead of solely using length changes to analyze shoreline diversity, and the length change intensity is applied to quantify the degree of shoreline change over time for different types of shorelines. Next, the composite index of coastline utilization degree is introduced to further explore the impact of human activities on shorelines. Then, to study the effect of coastal erosion on different types of shorelines in Fangchenggang, the end point rate is used to obtain the coastal erosion rate. Finally, the shoreline trend prediction model for Fangchenggang is established through the spatial distribution of the coastal erosion rate, and we verified that the accuracy of the model is 82%. The model can provide technical support for the integrated prevention and control of coastal erosion hazards.

1. Introduction

Coastal zones are important areas for the socioeconomic development of coastal countries and are the most active and frequent areas of human activity. Global climate change, sea level rise, and storm surges have increased the sensitivity of coastal areas to natural disasters,[1,2]

making coastal erosion hazards increasingly severe.[3–5] Therefore, coastal erosion status analysis and prediction are of great significance for economic development and environmental protection.

Fangchenggang City is near Beibu Gulf, with 10,000 square kilometers of ocean under its jurisdiction. It has a shoreline that makes up about 30% of Guangxi's mainland coast, stretching from Dongxing to Fangcheng and Gangkou districts. Fangchenggang has varied geomorphological features, with different types of shorelines. However, the shoreline has long been eroded because of the monsoon, storm surges, and other natural climatic factors.[6] At the same time, part of the Fangchenggang shoreline has also been affected by human activities such as land reclamation and sea enclosure, port construction, industrial development, and tourism.[7] The analysis and prediction of the coastal erosion status can provide not only support for ecological environmental protection and sustainable development of the city, but also a strong scientific basis for the management, protection, and governance of the shoreline.

Shoreline locations can be obtained by laser altimetry methods, such as light detection and ranging (LiDAR), which can delineate the location of the shoreline by determining elevation.[8] However, for complex terrains such as cliffs, caves, and steep rock walls, LiDAR may not be able to obtain complete and accurate shoreline data.[9] Therefore, it cannot be used as a reliable basis for shoreline location confirmation and further coastal erosion analysis. Aerial imagery is another method of mapping shoreline locations and is usually collected on a semi-regular basis. However, each image covers only a small area, and it is always collected along a flight path. Thus, adjacent images may have been collected on different dates or tidal cycles, resulting in data inconsistency.[10] This inconsistency has a significant impact on the determination of the shoreline location. In recent years, with the development of remote sensing technology, remote sensing images have been applied to shoreline dynamics and coastal erosion analysis with the advantages of wide monitoring range, high speed, low cost, and long-term dynamic monitoring on a large scale.[11–15] Do *et al.*[16] used satellite-derived shoreline time series and applied linear regression to estimate the rate of shoreline change as a means of understanding coastal erosion. Otmani *et al.*[17] used geographic information and digital shoreline analysis systems for data processing, shoreline change rate calculation, and coastal erosion change identification. Santos *et al.*[18] analyzed the mechanism of shoreline change in the Joao Pessoa area from both long-term and short-term perspectives, and discussed the relationship between the type of shoreline and sea level change.

Coastal erosion alters the topography, coastal structure, sea level, and human activities, which further leads to a change in the type of shoreline. Thus, a systematic analysis and prediction methods for coastal erosion state are studied. First, shoreline type changes are analyzed. The index of coastline type diversity (*ICTD*) is used instead of solely using length changes to analyze shoreline diversity, and the length change intensity (*LCI*) is applied to quantify the degree of shoreline change over time for different types of shorelines. Next, the composite index of coastline utilization degree (*ICUD*) is introduced to further explore the impact of human activities on shorelines. Then, to study the effect of coastal erosion on different types of shorelines in Fangchenggang, the end point rate (*EPR*) is used to obtain the coastal erosion rate. Finally, the shoreline trend prediction model for Fangchenggang is established

through the spatial distribution of the coastal erosion rate. The remainder of this paper is organized as follows. Materials and methods are presented in Sect. 2. The experiment and corresponding analysis are given in Sect. 3 to verify the effectiveness of the proposed method. Finally, conclusions are presented in Sect. 4.

2. Materials and Methods

2.1 Materials

2.1.1 Overview of study area

Located in the southern part of the Guangxi Zhuang Autonomous Region, Fangchenggang occupies the southwesternmost tip of the shoreline of mainland China. It is located roughly between 21°30'N and 22°25'N, and between 107°25'E and 108°40'E. The city has a length of 102 kilometers from north to south and a width of 116.8 kilometers from east to west, with a total area of 6,238.62 km^2. Fangchenggang is strategically located on the South China Sea coast, facing Haiphong City in Vietnam across the sea. It borders Vietnam to the southwest and serves as a key gateway for mainland China to Southeast Asia and the South Pacific Ocean. It offers convenient land and sea access to Southeast Asia and is the most direct route from southwest China to the Association of Southeast Asian Nations. At the same time, Fangchenggang has the largest port in western China, namely, Fangchenggang Port, which is an important land and sea transportation hub. It is also an important port for trade exchanges between China and Southeast Asian countries. The geographical location of Fangchenggang is shown in Fig. 1.
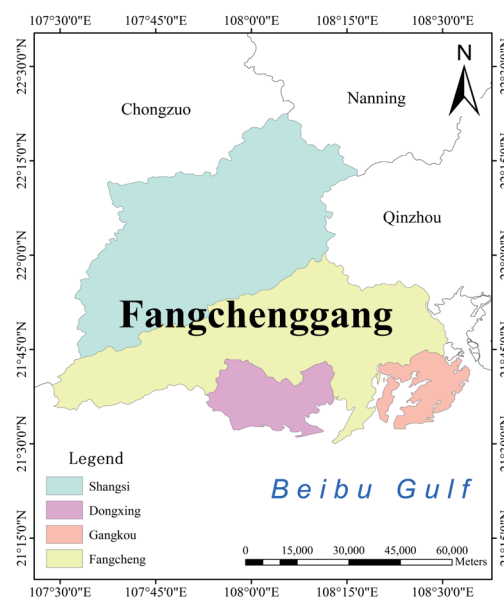

Fig. 1.   (Color online) Geographic location of Fangchenggang.

2.1.2 Data sources

To comprehensively assess the coastal erosion status of Fangchenggang, it is necessary to select the longest possible time span that can capture changes of the shoreline. Thus, in this study, a time span of approximately 30 years was chosen by extracting remote sensing images of the Fangchenggang shoreline for three different periods (1987, 2002, and 2019). To be more specific, Landsat-5 (1987), Landsat-7 (2002), and Sentinel-2 (2019) images of Fangchenggang were used. The 1987 data were chosen as the earlier reference data, and the data from 2002 and 2019 were selected as the comparison data to acquire the coastal erosion rates. This data selection can ensure the continuity and quality of the available data while capturing major shoreline trends. Moreover, the real shoreline extracted from Sentinel-2 images in 2023 around the Fangchenggang area was used as the reference to verify the effectiveness of our constructed shoreline prediction model. The Landsat series remote sensing data were from the Geospatial Data Cloud official website, and the Sentinel series remote sensing data were from the ESA Copernicus Data Center. The shoreline of Fangchenggang is guaranteed to be clearly visible in all the remote sensing images in order to increase the correctness of the shoreline discrimination to improve the accuracy of the experiment. The remote sensing images of Fangchenggang are shown in Fig. 2.
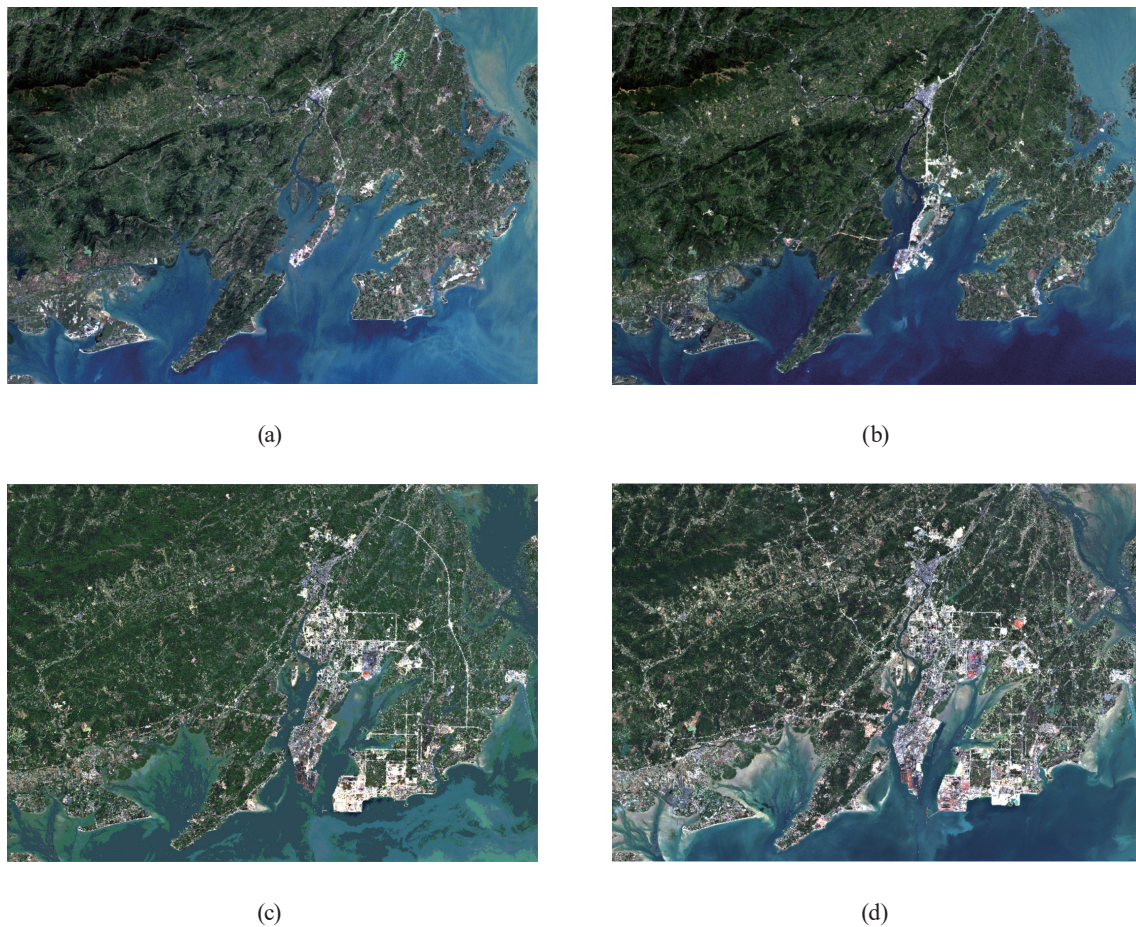

(a)

(b)

(c)

(d)

Fig. 2.　(Color online) Remote sensing images of Fangchenggang in (a) 1987, (b) 2020, (c) 2019, and (d) 2023.

2.2 Methods

Different types of shorelines have different formation mechanisms, and the texture characteristics shown on remote sensing images also differ. In this study, the shoreline information was first extracted by manual visual interpretation, which yields better results for the extraction of shoreline information in Fangchenggang, a large area with complex coastal development. According to the principles of defining and the remote sensing interpretation signs of different shorelines types, combined with the geomorphological features of the shoreline in the Fangchenggang area, the following five shoreline categories were identified and are shown in Fig. 3: sandy, silt, estuarine, bedrock, and artificial.

2.2.1 Methods for shoreline type change analysis

First, the length of the shoreline must be calculated to better understand the trend of the length change of the shoreline of Fangchenggang over the years. The length data calculation is also necessary to complete the statistics of shoreline total length change in different periods and the length change of each different type. However, there are many shortcomings in considering the shoreline type change from the perspective of length change alone. The most crucial point is that it is impossible to accurately judge the trend of shoreline type diversity owing to coastal erosion.[19] *ICTD* is a composite indicator used to measure the shoreline types diversity. It is used to assess the shoreline type diversity of a region by analyzing the proportion of different shoreline type diversity. *ICTD* can also offer a uniform index for shoreline type diversity, enabling direct comparisons over time and effectively identifying shoreline type diversity changes. Therefore, in this study, *ICTD* is applied to evaluate the shoreline type diversity:[19]

$$ICTD = 1 - \frac{\sum_i^n L_i^2}{\left(\sum_i^n L_i\right)^2},$$

(1)

where L_i is the length of the shoreline of the ith type and n is the number of shoreline division types. The *ICTD* range is always from 0 to 1. When the index is closer to 0, the shoreline types in the study area are more homogeneous, and when the index value is closer to 1, the diversity of each shoreline type is greater.

| (a) | (b) | (c) | (d) | (e) |

Fig. 3.   (Color online) Five types of shorelines: (a) sandy, (b) silt, (c) estuarine, (d) bedrock, and (e) artificial.

Then, to better compare the differences in shoreline type change in different periods, the *LCI* of the shoreline is also analyzed in this study; it can be expressed by adopting the average annual percentage length change. The *LCI* can quantify the intensity of the change in shoreline type per unit of time.[20] The formula is as follows:

$$LCI_{ij} = \frac{L_j - L_i}{L_i(j-i)} \times 100\%, \tag{2}$$

where LCI_{ij} denotes the intensity of shoreline type change from year i to year j. L_i denotes the length of a particular shoreline type in year i, and L_j denotes the length of a particular shoreline type in year j.

Moreover, the analysis of the reason for the shoreline type changes is also indispensable. Shoreline type changes are always affected by a variety of factors, including natural factors such as oceanic factors, riverine factors, and climate change, as well as anthropogenic factors resulting from human activities such as port construction, industrial development, and tourism. The effects of natural factors on the shoreline are usually slow, with a certain periodicity, and can reach a balance by itself within a certain range. Moreover, the effects of natural factors on shoreline type changes are usually scattered and random. In contrast, the effects of human factors on the shoreline are more direct, concentrated, and continuous, and they always increase with the frequency and intensity of human activities. To strengthen the quantitative analysis of the impact of human activities on the shoreline type changes, *ICUD* was calculated as shown in Eq. (3) using the human activity impact index. As shown in Table 1, different human activity indexes are assigned on different shoreline types in accordance with the degree of human activity impact on the shoreline.[21]

$$ICUD = \sum_{i=1}^{n} (A_i \times C_i) \times 100 \tag{3}$$

Here, n represents the number of shoreline types. A represents the index of the intensity of human activities corresponding to the ith-type shoreline. C represents the percentage of the length of the ith-type shoreline. The larger the *ICUD*, the more the shoreline is affected by human activities.

Table 1
Human activity impact index for different shoreline types.

Shoreline type	Human activity impact index
Sandy	2
Silt	3
Estuarine	1
Bedrock	1
Artificial	4

2.2.2 Spatial distribution of coastal erosion rates

It is essential to understand the location and severity of coastal erosion. In addition, the determination of the erosion spatial distribution is also necessary. Thus, in this study, *EPR* is applied to calculate the rate of coastal erosion in Fangchenggang. EPR is the ratio of the distance between the shoreline and its time interval in two phases and is used to study the changes in the type of shoreline in two different periods.[22] The *EPR* shown in Eq. (4) exhibits the advantages of low data requirements, rapid calculation, wide application range, and intuitive results. It enables the rapid and accurate assessment of coastal erosion changes.

$$EPR = \frac{D}{T} \tag{4}$$

Here, *D* represents the distance between the two shorelines and *T* represents the difference in time between the two shorelines.

To gain a clearer understanding of coastal erosion in Fangchenggang, the relationship between the erosion level and *EPR* is shown in Table 2. It can help to classify the erosion level, quantitatively assess the erosion rate, and obtain the spatial distribution image of coastal erosion rate in the study area.

2.2.3 Model construction for shoreline change prediction

To predict the future spatial distribution of the Fangchenggang shoreline, we established a prediction model on the basis of the *EPR* of the shoreline changes. The shoreline prediction model is constructed as follows:

$$\begin{cases} x = x_i + \dfrac{EPR \times \Delta t}{DIS} \times \left(x_i - x_j \right) \\ y = y_i + \dfrac{EPR \times \Delta t}{DIS} \times \left(y_i - y_j \right) \end{cases} \tag{5}$$

where *x* and *y* are the coordinates of the prediction points. x_i and y_i are the coordinates of the shoreline nodes in year *i*. x_j and y_j are the coordinates of the shoreline nodes in year *j*. Δt is the

Table 2
Relationship between erosion level and EPR.

Erosion level	*EPR* (m/year)
Severe erosion	$EPR \leq -3$
Aggressive corrosion	$-3 < EPR \leq -2$
Corrosion	$-2 < EPR \leq -1$
Microerosion	$-1 < EPR \leq -0.5$
Stabilization	$-0.5 < EPR \leq 0.5$
Oozing	$EPR > 0.5$

time difference between the predicted year and the initial year. *DIS* is the distance between the shoreline in year *i* and that in year *j*.

3   Experiment and Analysis

3.1   Spatial and temporal distributions of shoreline extraction

As shown in Fig. 4, the spatial locations of the Fangchenggang shoreline in 1987, 2002, and 2019 and the distribution information of each type of shoreline were obtained through visual interpretation. Among the shorelines considered, the artificial shoreline is red, the bedrock shoreline is yellow, the estuarine shoreline is blue, the silt shoreline is green, and the sandy shoreline is purple. This information is of considerable importance for studying the shoreline change trend, assessing the coastal erosion status and modeling the shoreline change trend.

It can be seen from Fig. 4 that during 32 years from 1987 to 2019, the shoreline with the widest distribution and the greatest change is the bedrock shoreline (in yellow). The shoreline with the highest growth rate is the artificial shoreline (in red). The sandy shoreline (in purple) also has a certain degree of growth, but not as fast as the artificial shoreline. The estuarine (blue) and silt (green) shorelines have changed negligibly in the 32-year study period.

To ensure the accuracy of the shoreline extraction results, 100 sample points were selected from three years of shoreline data. The accuracy was verified by calculating the distance from the predicted points to the real shoreline, and the distances from the predicted points to the required distances of the real shoreline were all within half a picture element. The error accuracy of the sample points from three years of shoreline data reached more than 90%.
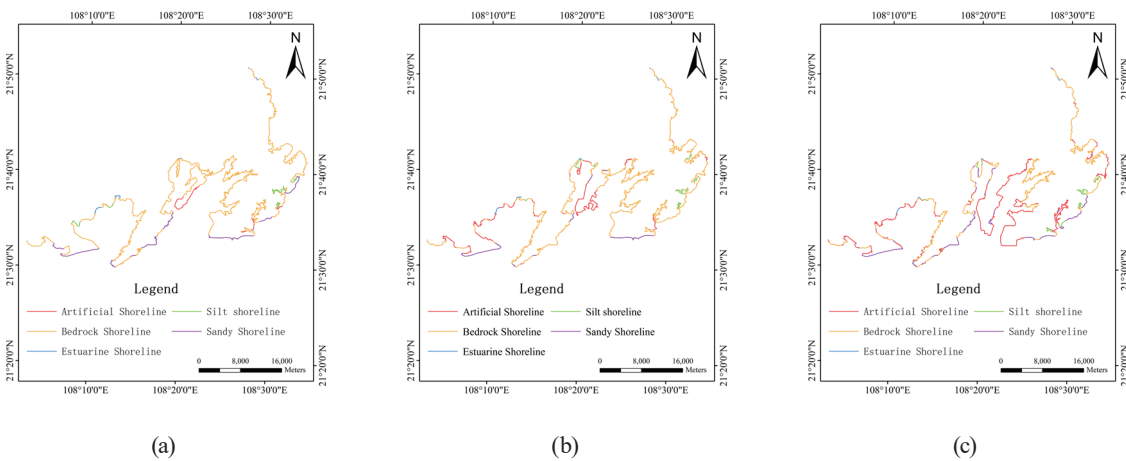

Fig. 4.   (Color online) Distribution of shoreline types in Fangchenggang in (a) 1987, (b) 2020, and (c) 2019.

3.2   Analysis of shoreline type changes

3.2.1   Analysis of shoreline length change and type diversity

Through the distribution information of each shoreline type in Fangchenggang, the total length of the shoreline and the length of each shoreline type in 1987, 2002, and 2019 were calculated. The curve of the shoreline length change is shown in Fig. 5. The shoreline length and length change statistics are shown in Tables 3 and 4, respectively. Moreover, the shoreline diversity is calculated for different years and shown in Table 5.

During 32 years from 1987 to 2019, the total length of the Fangchenggang shoreline increased yearly, while the changes were different for each shoreline type. The sandy shoreline showed a trend of first decreasing and then increasing. The length of the silt shoreline did not change significantly, but in general, it showed an increasing trend. The lengths of the estuarine and silt shorelines did not change significantly, but in general, they showed a decreasing tend yearly. The
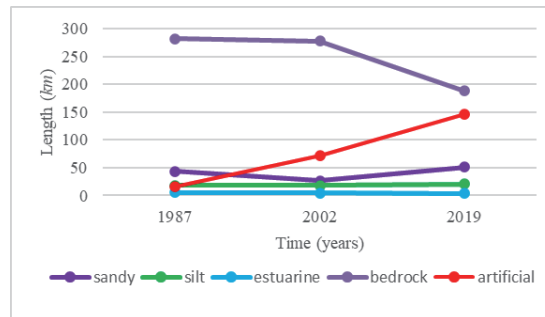

Fig. 5.   (Color online) Length change graph.

Table 3
Fangchenggang shoreline length statistics.

Particular year	Length (km)					
	Sandy shoreline	Silt shoreline	Estuarine shoreline	Bedrock shoreline	Artificial shoreline	Total length
1987	43.81	18.48	5.16	282.07	16.52	366.04
2002	26.52	18.47	4.81	277.05	71.46	398.31
2019	50.91	20.39	3.71	187.54	145.81	408.36

Table 4
Fangchenggang shoreline length changes statistics.

Particular year intervals	Change in length (km)					
	Sandy shoreline	Silt shoreline	Estuarine shoreline	Bedrock shoreline	Artificial shoreline	Total length
1987–2002	−17.29	−0.01	−0.35	−5.02	54.94	32.27
2002–2019	24.39	1.92	−1.10	−89.51	74.35	10.05
1987–2019	7.10	1.91	−1.45	−94.53	129.29	42.32

Table 5
Shoreline type diversity index in Fangchenggang.

Particular year	1987	2002	2019
ICTD	0.387	0.477	0.643

bedrock shoreline showed a trend of decreasing yearly, and the length of the artificial shoreline showed an increasing trend, which was the largest increase in length during the 32-year period from 1987 to 2019. The length of the artificial shoreline showed a yearly increase, and it was the shoreline with the largest increase in length over the 32-year period from 1987 to 2019. *ICTD* has been increasing during the 32-year period. The diversity index increased from 0.387 in 1987 to 0.477 in 2002 and finally to 0.643 in 2019. This is because the Fangchenggang shoreline is dominated by bedrock, but human activities have changed this situation. With the increase in human activity, the length of the artificial shoreline has been increasing and that of the bedrock shoreline has been decreasing, which affects the dominance of the bedrock shoreline. The Fangchenggang shoreline has changed from predominantly bedrock to the coexistence of artificial and bedrock shorelines, increasing the shoreline type diversity in Fangchenggang.

3.2.2 Shoreline change intensity analysis

By the analytical method discussed above, the intensity of each shoreline type change was analyzed in relation to that of total length change. The results are shown in Table 6 and Fig. 6.

It can be seen from the results that the total shoreline change intensity of Fangchenggang was always positive from 1987 to 2019. For each type of shoreline, the intensities of change for sandy and silty shorelines were initially negative and then positive, but the overall intensity of change was positive. The intensities of change for the estuarine and bedrock shorelines were always

Table 6
Shoreline change intensity statistics.

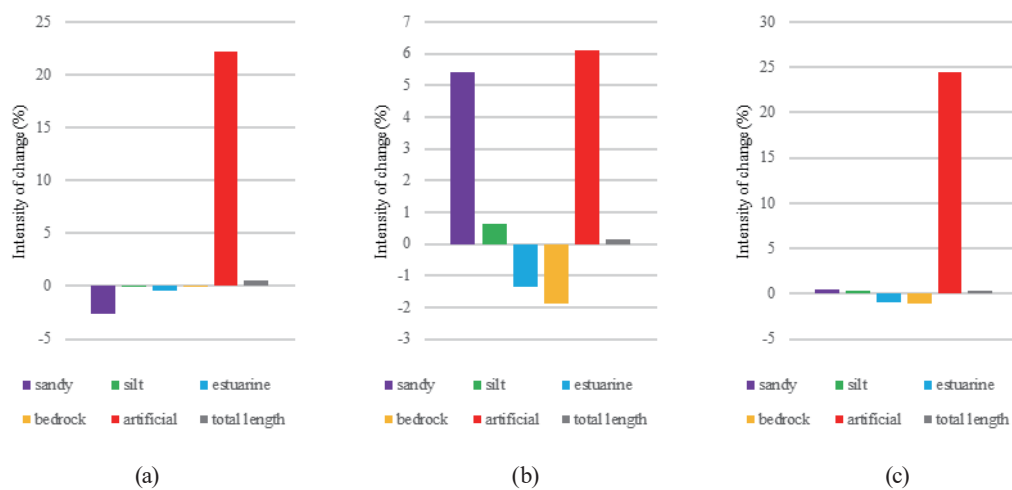| Year interval | Intensity of shoreline change (%) | | | | | |
	Sandy shoreline	Silt shoreline	Estuarine shoreline	Bedrock shoreline	Artificial shoreline	Total length
1987–2002	−2.631	−0.003	−0.452	−0.118	22.171	0.587
2002–2019	5.409	0.611	−1.345	−1.901	6.121	0.148
1987–2019	0.506	0.322	−0.878	−1.047	24.457	0.361

Fig. 6. (Color online) Histograms of shoreline change intensities at different year intervals: (a) 1987–2002, (b) 2002–2019, and (c) 1987–2019.

negative from 1987 to 2019, and the intensity of change for the artificial shoreline was always positive from 1987 to 2019, which indicated that human activities had the strongest impact. Moreover, the impact from 1987 to 2002 was more dramatic than that from 2002 to 2019.

3.2.3 Shoreline utilization analysis

The methodology described above was used to quantitatively analyze the impact of human activities such as port construction, industrial development, and tourism on coastal erosion, and the results are shown in Table 7.

As can be seen from the statistical results, *ICUD* in Fangchenggang has been increasing from 135.60 in 1987 to 169.75 in 2002, and then to 229.57 in 2019. This indicates that the effect of human activities on the state of coastal erosion is increasing. The composite index of shoreline utilization degree can be used to visualize the impact of human activities on coastal erosion. Over the past 30 years, the overall trend of ICUD has been increasing, which indicates that human activities have had a nonnegligible impact on coastal erosion in Fangchenggang.

3.3 Spatial distribution of coastal erosion rates

The spatial distribution of coastal erosion rates in different time periods in Fangchenggang was derived by the shoreline change EPR method, and the results are plotted in Fig. 7. Among them, severe erosion is shown in red, strong erosion in orange, erosion in yellow, microerosion in green, stabilization in blue, and siltation in purple.

Table 7
Impact index of human activities in Fangchenggang.

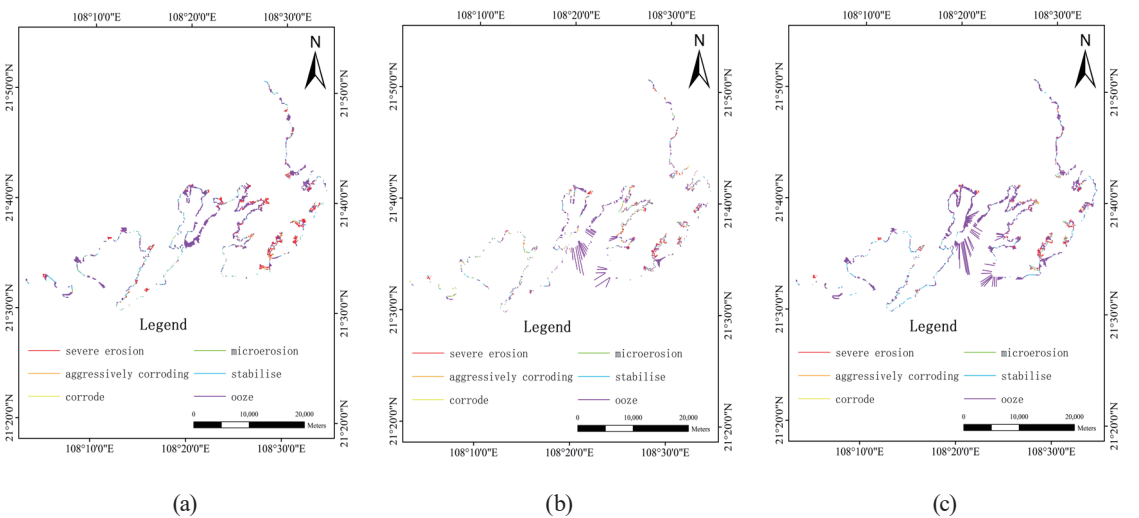| Particular year	1987	2002	2019
ICUD	135.60	169.75	229.57

Fig. 7. (Color online) Coastal erosion map of Fangchenggang at different year intervals: (a) 1987–2002, (b) 2002–2019, and (c) 1987–2019.

It can clearly be seen that the Fangchenggang shoreline shows expansion towards the ocean and an increasing land area during the 32-year period from 1987 to 2019. From 1987 to 2002, the coastal erosion in Fangchenggang was mainly dominated by siltation and supplemented by severe erosion. The siltation in the harbor area is the most obvious, but at the same time, the severe erosion is the most obvious also in the harbor area. From 2002 to 2019, the coastal erosion in Fangchenggang is mainly siltation. The siltation in the harbor area is the most obvious. Overall, the erosion in Fangchenggang from 1987 to 2019 was mainly siltation, and the area with the most significant siltation is the harbor district, which had significant siltation from 1987 to 2019. Thus, it can be concluded that the harbor district is the most dominant area of coastal erosion in Fangchenggang.

3.4 Prediction of shoreline changes

The predicted and real shorelines in 2023 are shown in Fig. 8. The predicted shoreline in 2023 was compared with the actual shoreline data acquired from the image of 2023 to verify the model's accuracy. The distance from the prediction point to the real shoreline must be kept within one image element, and the error accuracy is calculated to be 82%.

The shoreline situation of Fangchenggang in 2025 is predicted using the prediction model, as shown in Fig. 9. It can be seen that the Fangchenggang shoreline may expand more towards the ocean and the land area continues to increase. The most important expansion area is in the harbor area near the shoreline, which is basically consistent with the trend of coastal erosion
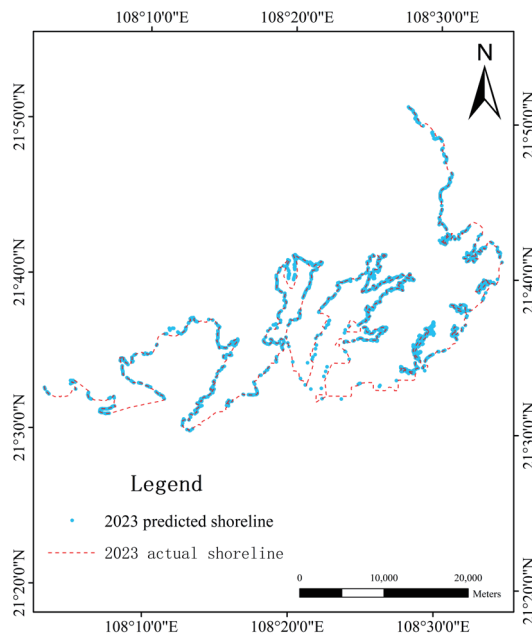

Fig. 8. (Color online) Actual and predicted shorelines of Fangchenggang in 2023.
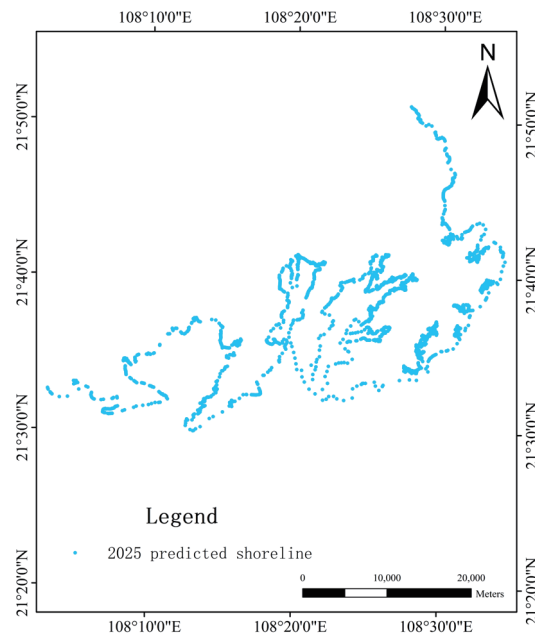
Fig. 9. (Color online) Predicted shoreline map of Fangchenggang in 2025.

between 1987 and 2019. The continued siltation of the shoreline of the port area is likely linked to the economic construction development in Fangchenggang. The results are projected using only past erosion rates and represent only the likelihood of future shorelines. The actual situation is more complex. The changes in shorelines are closely affected and determined by both the natural environment and human activities.

4. Conclusions

In this study, the coastal erosion changes in Fangchenggang were studied by analyzing Landsat TM and Sentinel-2 remote sensing images between 1987 and 2019. The total length of the Fangchenggang shoreline has been increasing during the 32-year period. The impact of anthropogenic activities on the shoreline has been increasing yearly, and the artificial shoreline has been growing and changing considerably. At the same time, because of human activities, the shoreline type diversity in Fangchenggang increased. The overall shoreline expanded toward the ocean, and the land area increased accordingly. In addition, a shoreline trend prediction model with a validation accuracy of 82% was established, which predicted that the shoreline will continue to expand in 2025, and the harbor area will be the main expansion area. This expansion will cause many problems such as coastal erosion, ecological damage, and the degradation of water quality. Therefore, development activities along the shoreline should be strictly controlled, and destructive development should be prohibited. At the same time, it is necessary to strengthen the protection and ecological restoration of offshore and shallow sea space.

The shoreline of Fangchenggang has changed considerably in 32 years, and the method proposed in this paper can yield results that better reflect the erosion status and future analysis of the shoreline of Fangchenggang. However, for areas where the coastal erosion is unclear, whether the method proposed in this paper is applicable needs to be proved by further experimentation in the future.

Acknowledgments

References

1 M. Becker, M. Karpytchev, and A. Hu: Nat. Clim. Change **13** (2023) 367. https://doi.org/10.1038/s41558-023-01603-w

2 T. H. J. Hermans, V. Malagón-Santos, C. A. Katsman, R. A. Jane, D. J. Rasmussen, M. Haasnoot, G. G. Garner, R. E. Kopp, M. Oppenheimer, and A. B. A. Slangen: Nat. Clim. Change **13** (2023) 359. https://doi.org/10.1038/s41558-023-01616-5

3 B. Guo and M. V. Subrahmanyam: Sens. Mater. **32** (2020) 3737. https://doi.org/10.18494/SAM.2020.2958

4 M. I. Vousdoukas, R. Ranasinghe, L. Mentaschi, T. A. Plomaritis, P. Athanasiou, A. Luijendijk, and L. Feyen: Nat. Clim. Change **10** (2020) 260. https://doi.org/10.1038/s41558-020-0697-0

5 G. Foti, G. Barbaro, G.C. Barillà, P. Mancuso, and P. Puntorieri: Eur. J. Remote Sens. **56** (2023) 2140076. https://doi.org/10.1080/22797254.2022.2140076

6　F. Aykut and D. Tezcan: Urban Inf. **1** (2024) 1. https://doi.org/10.1007/s41064-024-00284-0

7　H. Qiang and B. R. Silliman: Curr. Biol. **29** (2019) 1021. https://doi.org/10.1016/j.cub.2019.08.042

8　W. J. Schmelz and N. P. Psuty: Geomorphology **408** (2022) 108262. https://doi.org/10.1016/j.geomorph.2022.108262.

9　T. Klaas and S. Emeis: Wind Energy Sci. **2021** (2021) 1. https://doi.org/10.5194/wes-7-413-2022

10　A. E. Maxwell, T. A. Warner, B. C. Vanderbilt, and C. A. Ramezan: Photogramm. Eng. Remote Sens. **83** (2017) 737. https://doi.org/10.14358/PERS.83.10.737

11　L. Valderrama-Landeros, and F. Flores-de-Santiago: Ocean Coastal Manage. **169** (2019) 58. https://doi.org/10.1016/j.ocecoaman.2018.12.006

12　S. M. El-Hadidy: Arabian J. Geosci. **13** (2020) 1285. https://doi.org/10.1007/s12517-020-06229-2

13　M. E. Tapilatu, Y. Kaber, N. Alzair, H. Wona, K. C. Grady, and R. F. Tapilatu: Int. J. Environ. Sci. Technol. **20** (2022) 7007. https://doi.org/10.1007/s13762-022-04631-9

14　N. Depountis, D. Apostolopoulos, V. Boumpoulis, D. Christodoulou, A. Dimas, E. Fakiris, G. Leftheriotis, A. Menegatos, K. Nikolakopoulos, G. Papatheodorou, and N. Sabatakakis: J. Mar. Sci. Eng. **11** (2023) 654. https://doi.org/10.3390/jmse11030654

15　P. Nidhinarangkoon, S. Ritphring, K. Kino, and T. Oki: J. Mar. Sci. Eng. **11** (2023) 969. https://doi.org/10.3390/jmse11050969

16　A. T. Do, S. D. Vries, and M. J. Stive: J. Coastal Res. **35** (2019) 56. https://doi.org/10.2112/JCOASTRES-D-18-00021.1

17　H. Otmani, R. Belkessa, S. Bengoufa, W. Boukhediche, N. Djerrai, and K. Abbad: Arabian J. Geosci. **13** (2020) 124. https://doi.org/10.1007/s12517-020-5069-6

18　C. A. G. Santos, T. V. M. Nascimento, M. Mishra, and R. M. Silva: Sci. Total Environ. **769** (2021) 144889. https://doi.org/10.1016/j.scitotenv.2020.144889

19　L. Zhu, Z. Chu, K. Shen, E. Cui, and X Ma: Marine Geology Frontiers **38** (2022) 20. https://doi.org/10.16028/j.1009-2722.2021.080

20　J. Xu, Z. Zhang, X. Zhao, Q. Wen, L. Zuo, X. Wang, and L. Yi: J. Geogr. Sci. **24** (2014) 18. https://doi.org/10.1007/s11442-014-1070-x

21　L. Sui, J. Wang, X. Yang, and Z. Wang: Sustainablity **12** (2020) 3242. https://doi.org/10.3390/su12083242

22　S. C. Sam and B. Gurugnanam: Int. J. Environ. Sci. Technol. **20** (2023) 7463. https://doi.org/10.1007/s13762-022-04374-7